ChemComm

Accepted Manuscript

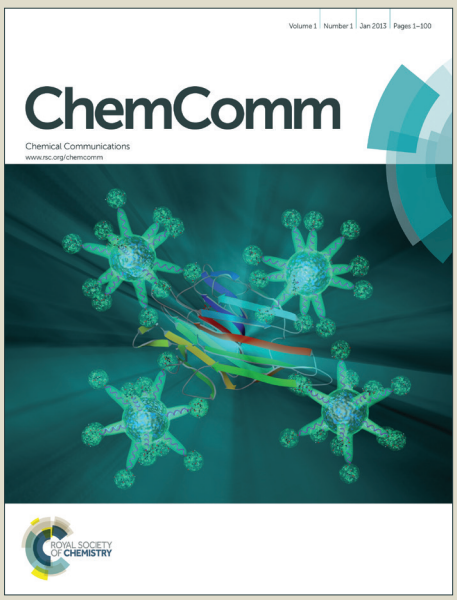

ROYAL SOCIETY OF CHEMISTRY

www.rsc.org/chemcomm

ChemComm

RSCPublishing

COMMUNICATION

Magnetic C-C@Fe_3O_4 double-shelled hollow microspheres *via* aerosol-based Fe_3O_4@C-SiO_2 core-shell particles

Cite this: DOI: 10.1039/xoxxoooooox

Received ooth January 2012,
Accepted ooth January 2012

DOI: 10.1039/xoxxoooooox

www.rsc.org/chemcomm

Yangzhi Zhu, Xiangcun Li*, Gaohong He, Xinhong Qi

Magnetic C-C@Fe_3O_4 hollow microspheres were prepared by using aerosol-based Fe_3O_4@C-SiO_2 core-shell particles as templates. The magnetic double-shelled microspheres were efficient in working as carriers to load Pt nanoparticles, making the catalyst recyclable and reusable.

Core-shell or core-shell-shell microspheres with magnetically response have recently attracted increasing attention due to their novel physicochemical properties with a large variety of applications in the fields of bioseparation and enrichment,[1] MRI contrast agent,[2] catalyst carries,[3, 4] and drug delivery.[5] Especially, Fe_3O_4/C composites have received much interesting as a result of tunable properties and chemically stable carbon materials, as well as significant synergetic or complementary interactions between Fe_3O_4 and carbon.[6]

Up to date, various methods including layer-by-layer coating process,[7] extended StÓber method,[8-10] Kirkendall effect,[11] and surfactant-templated method[12] have been reported for the synthesis of core-shell magnetic particles. However, the magnetic core is always encapsulated by several layers, which can shield or change the magnetic response of the core.[13] Magnetic separation can provide a convenient and low-cost method for the separation of solid particles in a multiphase suspension. Therefore, to improve their practical applications, considerable efforts have been devoted to enhance magnetic responsiveness of core-shell particles, and addition of new functionalities by combing with other functional nanomaterials.[6] Crystalline phase transition at high temperature, Ni modification etc. have been tried to enhance the magnetic responsiveness of the core-shell particles.[6, 14]

We report herein for the first time a rapid aerosol-based method for the preparation of Fe_3O_4@C-SiO_2 core-shell hollow particles and their transformation to C-C@Fe_3O_4 double-shelled magnetic microspheres. As illustrated in Schematic 1, the Fe_3O_4@C-SiO_2 template is simply obtained by a one-step aerosol strategy. The precursor solution containing appropriate ratio of Fe_3O_4 nanoparticles, TEOS, sucrose, CTAB, $FeCl_3$ and HCl was aerosolized and the resulting droplets passed through a heating furnace where hydrolysis and condensation of the precursors occurred to form spherical particles, a process similar to the synthesis of silica spheres in our previous reports.[15, 16] Then, a phenol resin layer was coated on the particle surface by a versatile in situ polymerization reaction. Magnetic C-C@Fe_3O_4 nanostructures were obtained by carbonization and selective removal of the silica. Obviously, the advantages of the study are as followings. First, the Fe_3O_4 cores encapsulated in the silica-carbon spheres are successfully transferred to the outer carbon shell of the double-shelled C-C porous particles, the novel idea largely increases the saturation magnetization value of C-C@Fe_3O_4 to 11.0 emu g^{-1}, compared to 2.9 emu g^{-1} for Fe_3O_4@C-SiO_2. This means that the novel nanostructure can be magnetically recycled when it is used as catalyst carries or bioseparation materials. The strategy by moving the Fe_3O_4 core to particle surface to enhance its magnetic responsiveness has not been reported previously. Second, 2,4-dihydroxybenzoic acid-formaldehyde (RF-COOH) instead of conventional phenol resin-formaldehyde (RF) is selected here.[17] The purpose is to form micelle clusters by electric attraction between negatively charged RF-COO^- group and cationic CTA^+ (CTA^+ B^-).[16] The CTAB clusters should be favorable to template large pores in the RF and carbon layer.[18] As expectedly, mesopores of ~50nm are obtained in the outer carbon layer of C-C@Fe_3O_4 microspheres. Interestingly, the Fe_3O_4 particles in the core are divided into smaller ones and embedded into the mesopores, which can be well preserved even etched in NaOH solution. Third, the Fe_3O_4@C-SiO_2 core-shell template can be prepared easily by a one-step aerosol process. The synthetic route reported here is expected to simplify the fabrication process of yolk-shell or double-shelled nanostructures, which usually entails multiple steps and a previously synthesized hard template.

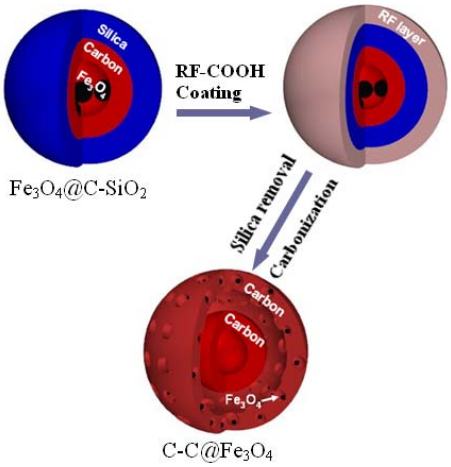

Schematic 1 Aerosol-based synthesis of Fe_3O_4@C-SiO_2 core-shell particles and their conversion to C-C@Fe_3O_4 porous microspheres with high saturation magnetization value

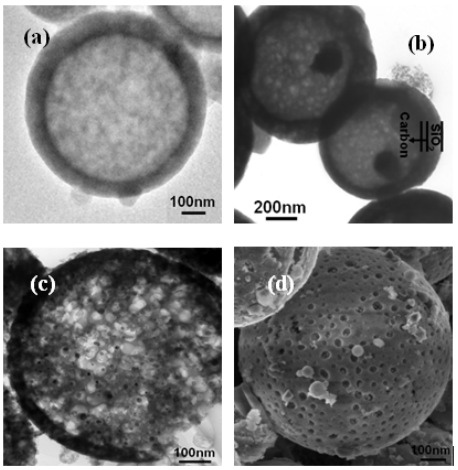

Fig. 1 (a) TEM image of C-SiO_2 hollow aerosol particles, (b) Fe_3O_4@C-SiO_2 core-shell aerosol particles, (c) (d) TEM and SEM images of C-C@Fe_3O_4 porous hollow particles.

Fig. 1a and b show TEM images of the C-SiO_2 and Fe_3O_4@C-SiO_2 core-shell particles synthesized based on a rapid aerosol method. The black spots can be ascribed to the encapsulated Fe_3O_4 nanoparticles in Fe_3O_4@C-SiO_2. The TEM images provide evidence of a double layer structure of the particles at progressively increasing resolution of the shell from the surface to inner layer.[15] Formation of the C-SiO_2 particles includes two steps: the generation of the silica layer due to the preferred silica condensation reaction along the gas-liquid interface of an aerosol droplet, sealing in the organic species in the particle interior. Subsequent pyrolysis in N_2 leads to a high internal pressure, forcing carbonaceous species against the silica wall to form an inner shell of carbon. Fortunately, the mechanism is also suitable in this study, and the Fe_3O_4 nanoparticles are successfully encapsulated into the hollow C-SiO_2 particles. The initially added ferric chloride in the aerosol solution has a crucial role on the formation of the hollow particles due to its salt bridging effect with CTAB, which has been fully studied in our previous works.[16, 18] The ferric chloride was transferred into Fe_3O_4 species during the carbonization process of the Fe_3O_4@C-SiO_2 aerosol particles in N_2 (Figure S3). EDS map (Fig. S5 A) of the inner carbon layer obtained by etching C-SiO_2 in HF clearly shows that the iron species are homogenously distributed in the shell (16.6 atomic %).

TEM and SEM images in Fig. 1c and d demonstrate the porous structure of the C-C@Fe_3O_4 particles, and the smaller Fe_3O_4 nanoparticles are well encapsulated into the pores. The double-shelled C-C structure and the outer porous carbon layer containing Fe_3O_4 nanoparticles are further confirmed by the broken spheres (Fig. S1c, d), compared with the relative smooth surface of the Fe_3O_4@C-SiO_2 particles (Fig. S1a, b). The HRTEM image also shows the encapsulation of Fe_3O_4 particles with ~10nm in the pores (Fig. S2), and the distance between two adjacent lattice planes is approximately 2.971Å, which corresponds to (220) lattice of Fe_3O_4 nanoparticles.[1]

It is known that there are possible interactions between carbon species and iron oxides under high-temperature conditions, where carbon species can induce carbothermic reduction to produce metal Fe, while iron oxides or Fe may promote the graphitization degree of carbon materials.[6] Therefore, it is primarily important to determine the crystalline phases of various composites. As shown in Fig. S3, the XRD peaks can be typically indexed to the Fe_3O_4 (JCPDS 02-1035), indicating the Fe_3O_4 phase can be well preserved during the carbonization process from Fe_3O_4@C-SiO_2 to C-C@Fe_3O_4. According to the HRTEM image (Fig.S4), graphitic carbon is observed around the Fe_3O_4 nanoparticles, because of the presence of the curved lattice fringes of graphitic layers.[19-21] These results suggest that chemical interactions between carbon species and iron oxides occur under current conditions (800℃, N_2 atmosphere). Zhang et al. reported that Fe_3O_4 core was converted into smaller Fe nanoparticles when the Fe_3O_4@PDA (polydopamine) core-shell particles were carbonized at 700 °C, leading to the fracturing and disappearance of the magnetic Fe_3O_4 cores, and the formed Fe nanoparticles were dispersed in the porous carbon shell.[19] However, in this study, Fe_3O_4 nanoparticles were found to be dispersed in the pores of outer carbon layer of C-C@Fe_3O_4 particles, with the disappearance of the Fe_3O_4 cores in Fe_3O_4@C-SiO_2 aerosol particles. Accordingly, we suppose that the Fe_3O_4 cores are fractured into smaller ones and dispersed in the pores during the carbonization process. The loose silica layer of the Fe_3O_4@C-SiO_2 hollow particles (Figure 1b) and the high pyrolysis pressure facilitate the movement of the fractured Fe_3O_4 core to the outer carbon shell of the double-shelled C-C porous particles.[15, 18] The presence of the silica layer can produce a passivating effect on the transformation of the Fe_3O_4 core into other Fe species.[6, 19, 22] The EDS map also shows the presence of the Fe_3O_4 core in Fe_3O_4@C-SiO_2, and homogeneous dispersion of iron species in C-C@Fe_3O_4 particles (Fig. S5 B, C). Controlled experiments reveal that both the CTAB and the Fe_3O_4 cores play important roles in generation of mesoporous carbon microspheres containing dispersed Fe_3O_4 nanoparticles (Fig. S6).

Fig. 2 shows that the saturation magnetization value of C-C@Fe_3O_4 is 11.0 emu g^{-1}, largely higher than the 2.9 emu g^{-1} for Fe_3O_4@C-SiO_2 and C-C microspheres. This can be ascribed to the transfer of Fe_3O_4 cores from C-SiO_2 interior to the outer porous carbon shell of C-C@Fe_3O_4, and the magnetic response can be mainly contributed to the dispersed Fe_3O_4 nanoparticles. For the C-C microspheres, the high temperature treatment (800℃) should largely improve the crystallinity (Figure S3) and magnetic response of the Fe_3O_4 species embedded in the inner carbon shell. This process makes the C-C microspheres showing a similar saturation magnetization value with the Fe_3O_4@C-SiO_2 hollow particles.

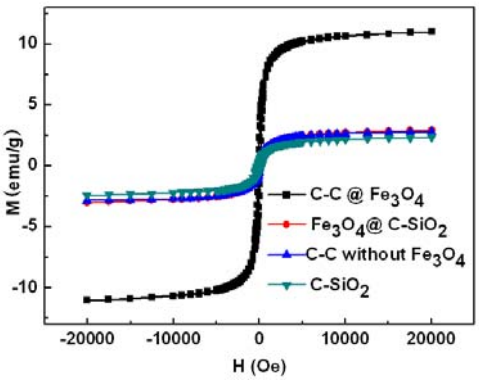

Fig. 2 Field-dependent magnetization curves of different samples, the saturation magnetization value reaches 11.0 emu g^{-1} for C-C@Fe_3O_4, compared to the 2.9 emu g^{-1} for Fe_3O_4@C-SiO_2.

The novel C-C@Fe_3O_4 nanostructure was used as carriers to load Pt nanoparticles (Fig. 3D, Fig. S5 D), and the reduction of 4-nitrophenol (4-NP) by $NaBH_4$ to 4-aminophenol (4-AP) was chosen as a model reaction to evaluate the catalytic capability of the C-C@Fe_3O_4-Pt composite. The reaction did not proceed without the presence of the catalyst. However, when the composite was added into the solution, the absorption at 400nm decreased quickly while the absorption at 295nm increased (Fig. 3A). The apparent rate constant k calculated from the $\ln(C_t/C_0)$ *vs.* time plot was 0.015 s^{-1} (Fig. 3B). The reduction of 4-NP into 4-AP was completed within 8min (Fig. 3C), the fast reaction of the 4-NP is believed to result from the highly dispersed Pt nanoparticles and high porosity of the carbon shell. The stability of the catalyst was investigated by repeating the reduction reaction with the same catalyst five times. After each reaction, the catalyst was recycled by an external magnetic field, followed by washing with ethanol and distilled water for several times. The catalyst showed high activity after 5 successive reaction cycles, with conversion near 100% within 8min. Clearly, the magnetic C-C microspheres were efficient in working as a carrier to load the Pt nanoparticles, making the catalyst recyclable and reusable. The results prove that the activity and stability of the C-C@Fe_3O_4-Pt composites are superior to those of the reported catalysts (Figure S7).[17, 23]

In summary, we have developed a facile aerosol-based approach to produce C-C@Fe_3O_4 magnetic microspheres, which is an ideal Pt nanoparticle carrier. The strategy here provides a simple and versatile synthetic approach toward designing magnetic yolk-shell or double-shelled C-C microspheres and therefore other various novel nanostructures for bioseparation, energy and environmental applications.

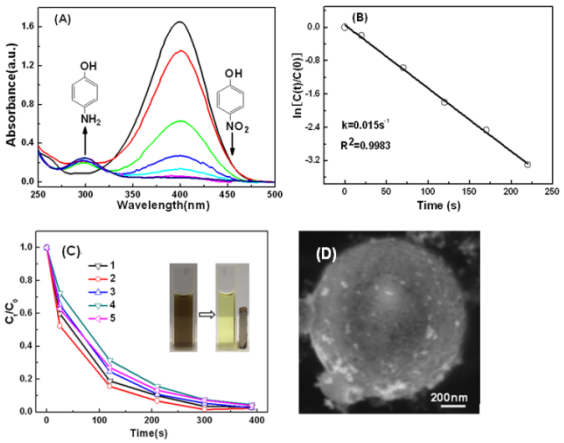

Fig. 3 Catalytic reduction of 4-NP in the presence of C-C@Fe_3O_4-Pt particles, (A) variation in UV-visible absorption spectra at different time intervals, (B) plot of $\ln(C_t/C_0)$ against the reaction time, (C) plot of C_t/C_0 against the reaction time in five successive cycles of the reduction reaction with the C-C@Fe_3O_4-Pt as the catalyst, (D) SEM image of the catalyst (20.3 wt.%, Pt).

We appreciate the financial support from Natural Science Foundation of China (21006008) and Fund for Distinguished Young Scholars of China (21125628).

Notes and references

State Key Laboratory of Fine Chemicals, Chemical Engineering Department, Dalian University of Technology, Linggong Road 2#, Dalian 116024, China. E-mail: lixiangcun@dlut.edu.cn.

† Footnotes should appear here. These might include comments relevant to but not central to the matter under discussion, limited experimental and spectral data, and crystallographic data.

Electronic Supplementary Information (ESI) available: [details of any supplementary information available should be included here]. See DOI: 10.1039/c000000x/

1 T. Yao, T. Cui, H. Wang, L. Xu, F. Cui and J. Wu, *Nanoscale*, 2014, **6**, 7666.
2 W. P. Li, P. Y. Liao, C. H. Su and C. S. Yeh, *J. Am. Chem. Soc.*, 2014, **136**, 10062.
3 J. Zhang, B. Li, W. Yang and J. Liu, *Ind. Eng. Chem. Res.*, 2014, **53**, 10629.
4 P. Zhang, R. Li, Y. Huang and Q. Chen, *ACS Appl Mater Interfaces*, 2014, **6**, 2671.
5 C. Yang, W. Guo, L. Cui, N. An, T. Zhang, H. Lin and F. Qu, *Langmuir*, 2014, **30**, 9819.
6 Y. Du, W. Liu, R. Qiang, Y. Wang, X. Han, J. Ma and P. Xu, *ACS Appl Mater Interfaces*, 2014, **6**, 12997.
7 Y. Xie, B. Yan, H. Xu, J. Chen, Q. Liu, Y. Deng and H. Zeng, *ACS Appl Mater Interfaces*, 2014, **6**, 8845.
8 Y. Deng, Y. Cai, Z. Sun, J. Liu, C. Liu, J. Wei, W. Li, C. Liu, Y. Wang and D. Zhao, *J. Am. Chem. Soc.*, 2010, **132**, 8466.
9 W. Hu, B. Liu, Q. Wang, Y. Liu, Y. Liu, P. Jing, S. Yu, L. Liu and J. Zhang, *Chem. Commun.*, 2013, **49**, 7596.
10 L. Li, Y. Feng, Y. Li, W. Zhao and J. Shi, *Angew. Chem. Int. Ed.*, 2009, **48**, 5888.

11 F. Liu, J. Zhu, W. Yang, Y. Dong, Y. Hou, C. Zhang, H. Yin and S. Sun, *Angew. Chem. Int. Ed.*, 2014, **53**, 2176.
12 M. Wang, X. Wang, Q. Yue, Y. Zhang, C. Wang, J. Chen, H. Cai, H. Lu, A. A. Elzatahry, D. Zhao and Y. Deng, *Chem. Mater.*, 2014, **26**, 3316.
13 H. Zhang, X. Li, G. He, J. Zhan and D. Liu, *Ind. Eng. Chem. Res.*, 2013, **52**, 16902.
14 M. Sanles-Sobrido, M. Perez-Lorenzo, B. Rodriguez-Gonzalez, V. Salgueirino and M. A. Correa-Duarte, *Angew. Chem. Int. Ed.*, 2012, **51**, 3877.
15 Y. Wang, B. Sunkara, J. Zhan, J. He, L. Miao, G. L. McPherson, V. T. John and L. Spinu, *Langmuir*, 2012, **28**, 13783.
16 X. Li, V. T. John, G. He, J. He, and L. Spinu, *J. Mater. Chem.*, 2012, **22**, 17476.
17 R. Liu, F. Qu, Y. Guo, N. Yao and R. D. Priestley, *Chem. Commun.*, 2014, **50**, 478.
18 X. Li, V. T. John, J. Zhan, G. He, J. He and L. Spinu, *Langmuir*, 2011, **27**, 6252.
19 G. Cheng, M. D. Zhou and S. Y. Zheng, *ACS Appl Mater Interfaces*, 2014, **6**, 12719.
20 H. Geng, Q. Zhou, Y. Pan, H. Gu and J. Zheng, *Nanoscale*, 2014, **6**, 3889.
21 J. Sanetuntikul, T. Hang and S. Shanmugam, *Chem. Commun.*, 2014, **50**, 9473.
22 L. Liang, Q. Zhu, T. Wang, F. Wang, J. Ma, L. Jing and J. Sun, *Microporous Mesoporous Mater.*, 2014, **197**, 221.
23 X. Wen, G. Li, Q. Chen, H. Zhang, X. Ba and G. Bai, *Ind. Eng. Chem. Res.*, 2014, **53**, 11646.